The Journal of Engineering Geology, Vol.9, No.3, December, 1999, pp.243-251

水浸삼축압축하에서 관찰되는 화강암의 미세 파괴

Micro-damage Process in Granite Under the State of Water-saturated Triaxial Compression

서 용 석 (Yong Seok Seo) 경북대학교 자연과학대학 지질학과
정 교 철 (Gyo Cheol Jeong) 안동대학교 자연과학대학 지구환경과학과

요약 / ABSTRACT

일반적으로 등방·균질 재료로 취급되고 있는 화강암 내에는 많은 미세 결함들이 존재한다. 암석에서 이들 미세 결함들이 단계적으로 발생, 진전하여 취성파괴가 일어나는 것으로 알려져 있다. 본 논문에서는 새롭게 개발된 시험기를 이용하여 水浸삼축압축시험중에 일어나는 微小크랙의 발생, 진전 및 상호작용을 연속적으로 관찰하고, 그 형태를 분류하였다.

주요어 : 화강암, 미소결함의 진전과정, 연속 및 동시관찰

Granitic rock, by its nature, contains numerous micro-discontinuities including grain boundary, microcracks, microcavities and mineral cleavages. The brittle fracture of rock is a progressive procedure in which the failure occurs with prior microcracking. In this paper, initiation, propagation and interaction of microcracks are considered to be the dominant, controlling micromechanisms of macroscopic failure. The authors show a few patterns of microcrack initiation and propagation by using sequential photographs of water-saturated granite taken under triaxial compressive state. The failure process was observed directly and continuously by a newly developed triaxial compressive test system.

Key Words : Granite, Synoptic observation, micro-damage process, sequential photographs

1. INTRODUCTION

Recently in engineering application of rock mechanics for mining, petroleum and nuclear industries, difficult excavation works are carried out at large depth. In these works a failure analysis around the underground opening in stressed rock mass is important for the practical reason of stability and safety. Granite, as a most natural rock, is characterized by microstructures including microcracks and grain boundaries whose evolution and interaction, called the micro-damaging process determine their macroscopic mechanical response. The constituent minerals and their preferred orientation do not only affect the physical properties of granite. The arrays of numerous small defects that are oriented preferentially also affect the physical properties of granite (Yukutake, 1989; Jeong and Ichikawa, 1994). Many experimental studies in postloaded samples relating to damage propagation problem have shown that macroscopic fractures grow from grain-scale microcracks that are abundantly found in crystalline rocks (Peng and Johnson, 1972; Wong, 1982; Mardon et al, 1990). But, most of them have disadvantage of having been performed only under zero stress condition using thin or cut section after experiment, or under artificially fractured conditions.

To better understand the fundamental problem of true damage process of microscale to macroscale in coarse-grained specimen under the state of water-saturated triaxial compressive stress, we developed a new experimental system that allows us to observe the actual micro-damage process during the deformation of specimens. By using the system we carried out a series of triaxial compressive test to observe continuously damaging process under loading for the same specimen. In this study, we supposed a perfectly saturated rock mass by groundwater.

2. EXPERIMENTS

2.1 Specimen

It is well known that most granites are characterized by a microcrack fabric that allows quarrymen to split the granite in a consistent and predictable manner (Bell, 1936; Wise, 1964; Chen et al., 1997). Quarrymen refer to the three easiest directions of splitting as rift, grain and hardway in order of ease of splitting. The specimen used in this study are coarse-grained granite of Late Cretaceous to Early Paleogene (about 60 million years), distributed in the Tsukuba area, Japan (Takahashi, 1982). We call this Inada granite in this study. Table 1 shows

Table 1. Model composition and physical properties of Inada granite.

Components	Properties
Quartz (Q)	27.8 %
Feldspar (F)	63.1 %
Mica	9.0 %
Others*	0.1 %
Color	Greyish white
Texture	Equigranular
Grain size of Q and F	3-8 mm

*Others: Zircon and apatite, etc.

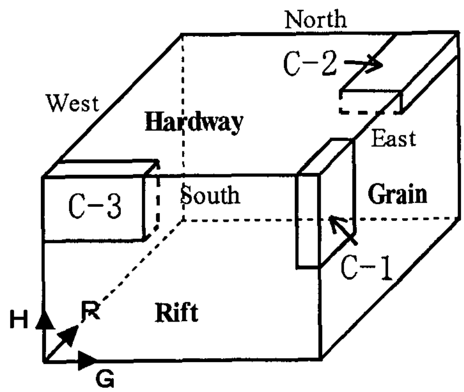

Fig. 1. Oriented specimen preparation for laboratory test.

modal composition and physical properties of Inada granite. Specimens were made to involve three mutually perpendicular cleavages as of rift, grain and hardway plane shown in Fig. 1. The dimensions of a specimen is 40×20×5mm. All of the samples are prepared to ensure a tolerance of 4/1000mm concerning parallelism and perpendicularity of the faces. The observing surface is polished by 1000 gr. emery powder for the purpose of easy observation by microscope.

2.2 Experimental system

To observe actual propagation of microcracks and its effect to the macroscopic response of the rock material under triaxial compressive state, a new testing system shown in Fig. 2 is developed. The experimental system consists of three subsystems: a) the loading system, b) the data-recording system and c) the observation system. The data-recording system is composed of an A/D transducer and personal computer. The observation system includes a stereoscopic microscope (Nikon, SMZ-U) with magnifying power of 110 times, a still camera, a CCD video camera with a TV monitor and a ring type lighter (NPI, PLG-TR32). The microscope can be moved to observe a wide surface of specimen on an X-Y stage and sequential photographs can be taken. The loading system allows us to observe the surface of specimen under states of uniaxial and triaxial compression. It consists of a vessel, an axial loading pump, an oil jack, a piston, a loading platen and a load cell (Tokyosoki, DM6820) which is originally designed by the authors. A lid including windows for observation, a pump for confining pressure (Japan Precision Science, NPL-5000), a regulator (Tescom, 26-1700) and two tanks are used additionally for triaxial compressive test.

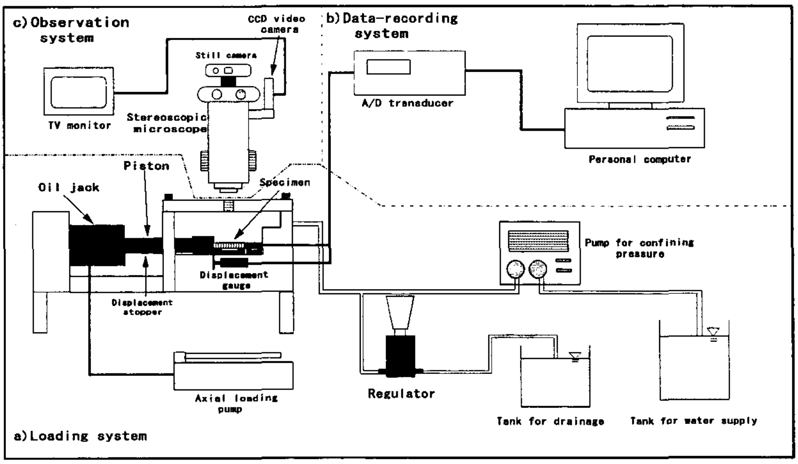

Fig. 2. Schematic diagram of experimental System.

2.3 Experimental procedure

The testing procedure is summarized as follows: First, a specimen is placed on a concave-shaped steel block that is put on the bottom surface of the vessel. Next, a load is applied to the specimen at the rate of 0.2MPa/sec by using a manually controlled pump. For the triaxial tests, confining pressure is applied concurrently with axial pressure as the same velocity to a specified stress level by using the pump for confining pressure and regulator. The axial pressure is applied to the stress level of failure.

3. RESULTS AND DISCUSSION

3.1 Anisotropy of strength

One can generally assume an isotropic behavior in considering failure condition of rock. This assumption is only valid for rocks that do not have a preferred orientation of discontinuities or other distinctive fabric (Kudo et al., 1986; Lee and Park, 1993). The influence of cracks on its strength is generally very strong even if in dry condition. When the cracks are filled with a fluid of relatively low compressibility, such as liquid water, the effect of the cracks in reducing shear strength increase more significantly(Seo et al., 1999).

We carried out water-saturated triaxial compressive tests of 5 samples for each type of specimens. Figure 3 shows distribution of mean compressive strengths of Inada granite tested under water-saturated uniaxial (Seo et al., 1999) and triaxial compression. The result shows that C-2 type specimens give about 15-20 MPa higher uniaxial and triaxial strengths than other ones. The results may be influenced significantly by anisotropic distribution of preferred cracks in specimen. In the previous paper, it was revealed

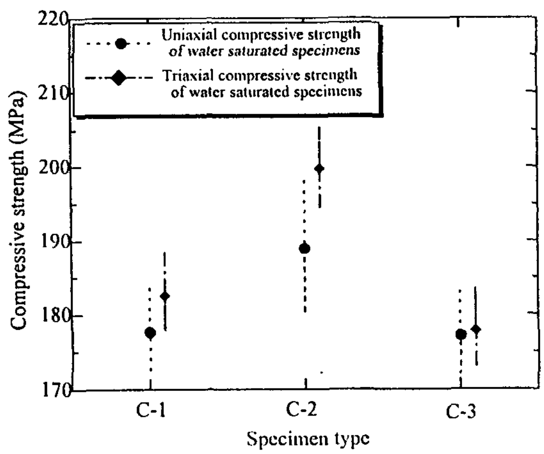

Fig. 3. Distribution of compressive strengths of Inada granite.

that microcrack density of Inada granite varies according to the measuring direction. For instance, C-2 samples that show the highest average strength in wet state are made parallel to the hardway plane, and their density of microcrack extended to the loading direction is lower than those of other specimen. The interstitial fluid through chemical or other processes may also have an active role for a specific weakening of a rock strength (Parate, 1973). According to Martin(1972) water break Si-O bonds in silicate rocks as a chemical role.

3.2 Synoptic observation of micro-damage process

It is generally found that the stress-strain behavior deviate from elastic behavior, prior to the macroscopic failure, in the higher part of the differential load range. Such inelastic effects are known to be resulted from microcracking. The failure of brittle rocks has been investigated by many researchers (Hoek and Bieniawski, 1965; Brace et al., 1966; Bieniawski, 1967; Scholz, 1968; Wawersik and Fairhurst, 1970; Wawersik and Brace, 1971; Peng and Johnson, 1972; Tapponnier and Brace, 1976). According to these researches, the stress-strain behavior of the rock in compression can be divided into several stages prior to the macroscopic fractures as shown in Fig. 4. Strains were measured by using waterproof strain gauges (Tokyosoki, WFLA-3).

Stage I is the initial region of the stress-strain curves in which the closure of existing microcracks in the specimen. It depends on the initial crack density and crack geometry whether the closure is present or not.

Stage II is thought as linear, homogeneous, elastic region. There is no evidence of microcrack development. From the stress-strain curve the elastic properties is calculated in this region.

In Stage III, dilatancy is clearly appeared with initiation and propagation of large numbers of microcracks parallel to the direction of the maximum principal compressive stress. The

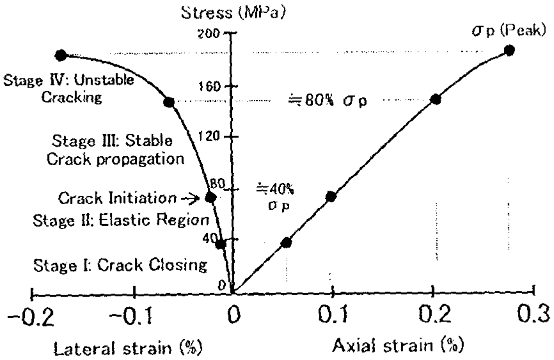

Fig. 4. Stress-strain diagram obtained from a triaxial compressive test for Inada granite showing crack development demarcation of four stages.

microcrack propagation is distributed fairly and uniformly throughout the specimen.

Stage IV represents the onset of marked localization' of the microcrack growth and the complete progression to macroscopic fracture. There are two failure types. One is that microcracks continue to be axial in orientation, and the other is that an increasing proportion comes to be of inclined orientation or shear direction. The development of crack is unstable and inhomogeneous in this stage.

The results of direct observations of significance on the detail of the process of brittle failure in rock under the state of triaxial compressive stress are introduced. These observations have been carried out at various points on the pre-failure stress-strain curve

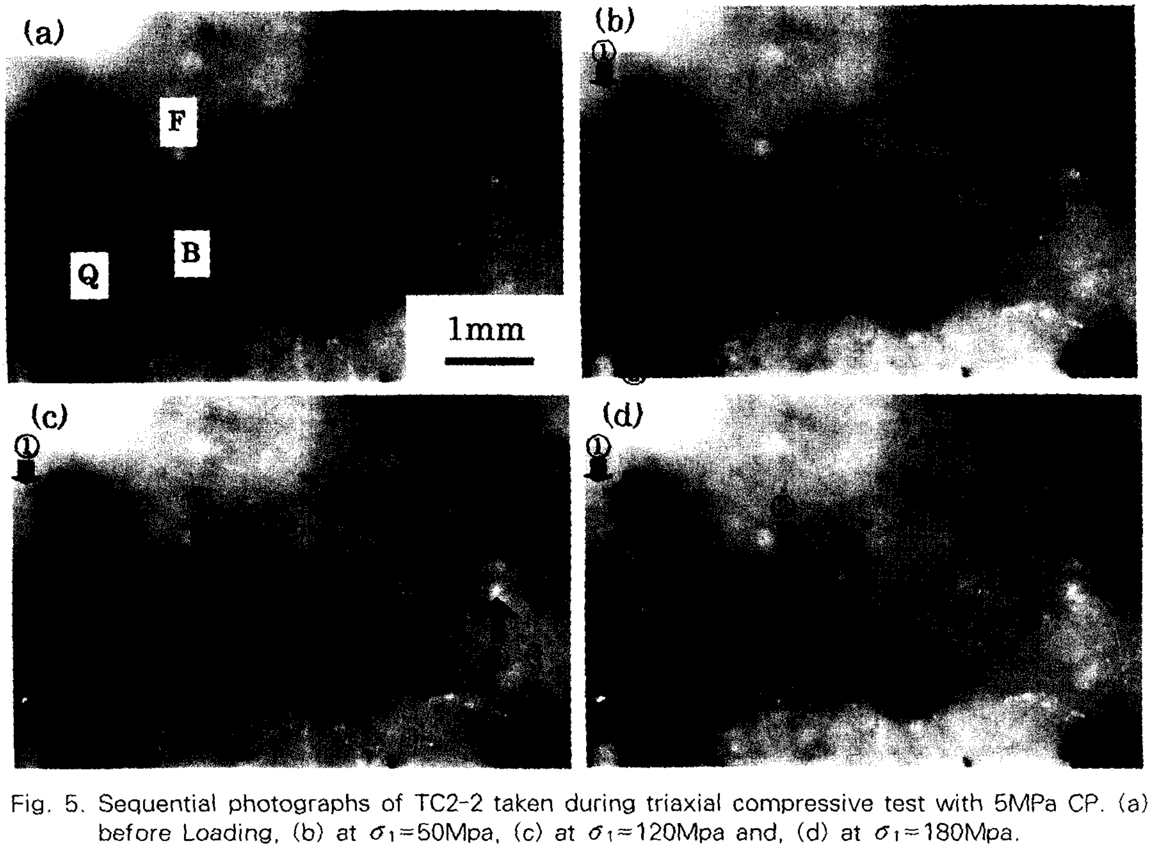

Fig. 5. Sequential photographs of TC2-2 taken during triaxial compressive test with 5MPa CP. (a) before Loading, (b) at σ_1=50Mpa, (c) at σ_1=120Mpa and, (d) at σ_1=180Mpa.

under 5MPa confining pressure. The direction of loading is horizontal in all tests.

The sequential photographs of TC2-2 specimen that failed at 199MPa of axial stress are shown in Fig. 5 (a)-(d). TC2-2 means the second C-2 type specimen tested under triaxial compression. Fig. 5 (a) was taken before loading, and we can observe the essential rock-forming minerals such as quartz (Q), feldspar (F) and biotite (B). G.B. also means grain boundary here. Pay attention to the mark of ←X. One is able to find the microcrack closing in Fig.5 (b) with increasing the axial loading. Transgranular cracking in feldspar at biotite G.B. begins at the mark of ① → in Fig. 5 (b) and propagate largely in Fig. 5 (c) and (d). Marks of ②③→ point out tension crack propagation of pre-existing cracks and G.B.s parallel to the loading direction together in Fig. 5 (b), (c) and (d). The path of cracking that is usually horizontal is curved along the biotite G.B. when the intracrystalline microcrack meets biotite G.B. (see the mark of ③→).

Figure 6 (a)-(d) show the sequential photographs of TC3-2 specimen that failed at 177MPa of axial stress. Hardway planes are found in Fig. 6 (a). Transgranular crack is developed in quartz starting from biotite G.B., indicated by the mark of ③→ at σ_1 =120MPa in Fig. 6 (c). It is going to grow longer at σ_1=170MPa in Fig. 6 (d). Intersection of G.B. of quartz and feldspar are indicated by the mark of ←① in Fig. 6 (b). This G.B. crack marked with

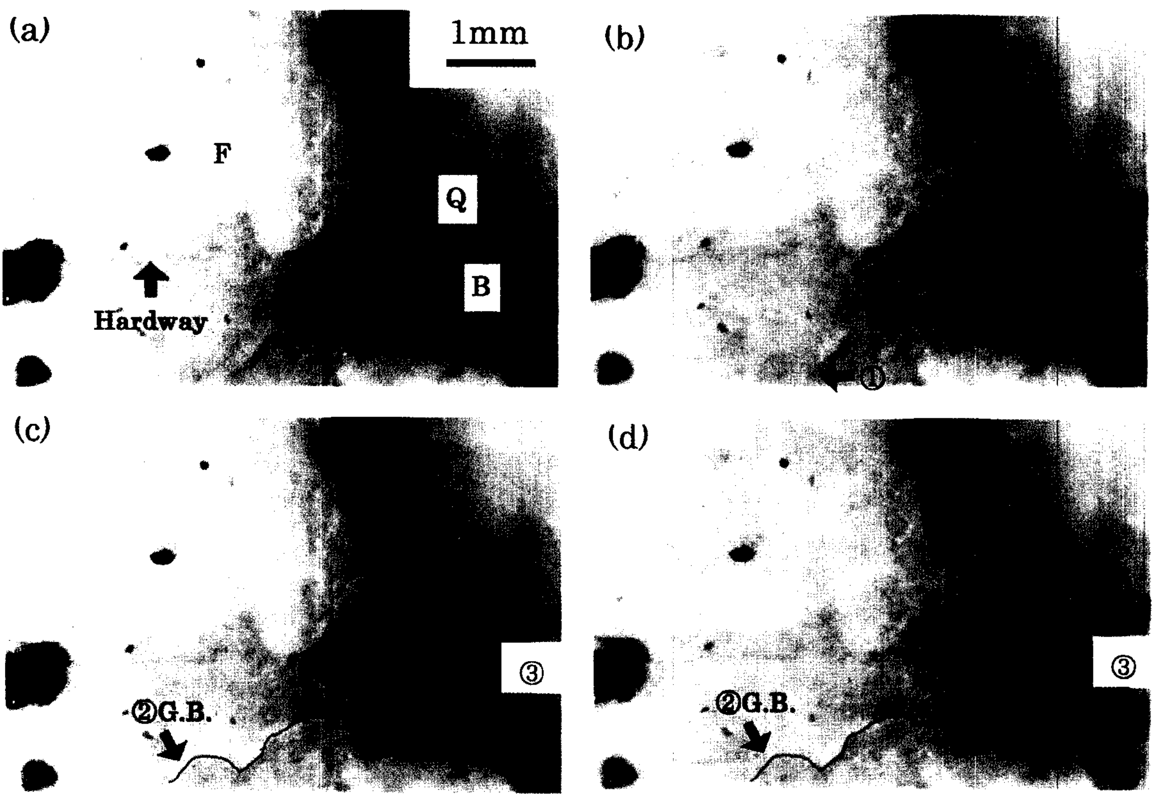

Fig. 6. Sequential photographs of TC3-2 taken during triaxial compressive test with 5MPa CP. (a) before loading, (b) at σ_1=50Mpa, (c) at σ_1=120Mpa and, (d) at σ_1=170Mpa.

②→ is developed to the loading direction as shown in Fig. 6 (c) and (d).

Four models of microcracking which are schematically drawn in Fig. 7 are postulated on the basis of these sequential photographs.

(a) Transgranular cracking in quartz or feldspar at biotite grain boundary: Fresh cracks appear in the boundary of biotite.

(b) Microcrack closing in quartz or feldspar: This occurs at the initial stage of loading. In this study, longitudinal cracks are particularly closed with increasing load in quartz.

(c) Intersection of inclined biotite and G.B.s of another mineral: Frictional sliding seems to be developed along the boundary of biotite with surrounding grains when a biotite cleavages oriented at relatively high angle to the axial load direction. It is sometimes observed at grain boundary of the same minerals such as feldspar and quartz.

(d) Tension of pre-existing cracks and grain boundary: It is mostly predominant cracking throughout the specimens. Microcracks are developed toward the orientation parallel to the load direction but some microcracks are inclined up to 30° or more to the load direction.

The same models appeared in the result of uniaxial compressive tests (Seo, et al.,1999). But crack propagation rate in granite may be increased under the much higher confining pressure by the increasing effective stress which occur because of the independent pores.

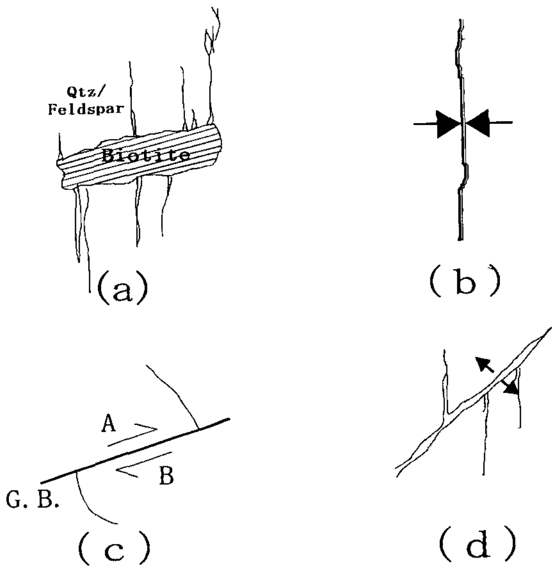

Fig. 7. Idealized sketches of microcracks resulting from application of load in Inada granite, as revealed by stereoscopic microscope. (a) Transgranular cracking in quartz or feldspar at biotite grain boundary (Tapponier and Brace, 1976). (b) Microcrack closing in quartz or feldspar. (c) Intersection of inclined biotite and G.B.s of another mineral (Olsson and Peng, 1976). (d) Tension of pre-existing crack and grain boundary.

4. CONCLUSIONS

In crystalline rock there are numerous complex mechanisms which may be responsible for microcracking. In this paper, synoptic observations in granite show that initiation, propagation and interaction of micro-defects such as pre-existing microcracks and grain boundaries are the dominant micro-events that lead to macroscopic fracture and failure of rock under triaxial compression. And four models of microcracking could be identified on the basis of observing sequential photographs taken under water-saturated triaxial compression.

REFERENCES

Bell, J. F., 1936, The investigation of the cleavage of granite, Econ. Geol., 31, 72-277.

Bieniawski, Z. T., 1967, Mechanism of brittle fracture of rock, parts I, II and III, Int. J. Rock. Mech. Min. Sci., 4, 395-430.

Brace, W. F., Paulding, B. W. Jr., and Scholz, C., 1966, Dilatancy in the fracture of crystalline rocks, J. Geophys. Res., 71, 3939-3953.

Chen, Y., Nishiyama, T., Kita, H. and Sato, T., 1997, Correlation between microfracture type and splitting planes of Inada granite and Kurihashi granodiorite, J. Japan Soc. Eng. Geol., 38, 196-204.

Hoek, E. and Bieniawski, Z. T., 1965, Brittle fracture propagation in rock under compression, J. Fracture Mech., 1, 137-155.

Jeong, G. and Ichikawa, Y., 1994, An experimental study on damage propagation of intact granite, J. Materials Sciences, Japan, 43, 317-323.

Kudo, Y., Hashimoto, K., Sano, O. and Nakagawa, K., 1986, Relation between physical anisotropy and microstructure of granite, J. Japan Soc. Civ. Eng., 370, III-5, 189-198 (in Japanese).

Lee, S. and Park, H., 1993, Preferred orientation and anisotropy of 'Rift' within granites in the quarrying fields, J. Korean Inst. Min. Energy Resou. Eng., 30, 6, 463-468 (in Korean).

Mardon, D., Kronenberg, A. M., Handin, J., Friedman, M., and Russel, J. E., 1990, Mechanisms of fracture propagation in experimentally extended Sioux Quartzite, Tectonophysics, 182, 259-278.

Martin, R. J., 1972, Time-dependent crack growth in quartz and its application to the creep of rocks, J. Geophys. Res., 77, 1406-1419.

Olsson, W. A., and Peng, S., 1976, Microcracks nucleation in marble, Int. J. Rock Mech. Min. Sci. Geomech. Abstr., 13, 53-59.

Parate, N. S., 1973, Influence of water on the strength of limestone, Trans. A. I. M. E., Soc. Min. Eng., 254, 127-131.

Peng, S., and Johnson, A. M., 1972, Crack growth and faulting in cylindrical specimens of Chelmsford granite, Int. J. Rock Mech. Min. Sci., 9, 37-86.

Scholz, C. H., 1968, Experimental study of the fracturing process in brittle rocks, J. Geophys. Res., 73, 1447-1453.

Seo, Y. S., 1999, Damage Process in Granite: Experimental Observation, Molecular Dynamics Simulation and its Homogenization Analysis, Nagoya University, Ph. D. thesis, 28p.

Seo, Y. S., Seiki, T. and Ichikawa, Y., 1999, Crack generation and propagation during stress relaxation of crystalline rock under water-saturated uniaxial condition, J. Soc. Materials Science, Japan, 48, 11, 1255-1262 (in Japanese).

Takahashi, Y., 1982, Geology of the granitic rocks in the Tsukuba area, J. Geol. Soc. Japan, 88, 177-184.

Tapponier, P. and Brace, W. F., 1976, Development of stress-induced microcracks in Westerly granite, Int. J. Rock Mech. Min. Sci. Geomech. Abstr., 13, 103-112.

Wawersik, W. R. and Brace, W. F., 1971, Post-failure behavior of a granite and diabase, Rock Mech., 3, 61-85.

Wawersik, W. R., Fairhurst, C., 1970, A study of brittle rock fracture in laboratory compression experiments, Int. J. Rock Mech. Min. Sci., 7, 561-575.

Wise, D. U., 1964, Microjointing in basement, middle Rocky mountains of Montana and Wyoming, Geol. Soc. Am. Bull., 75, 287-292.

Wong, T. F., 1982, Micromechanics of faulting in Westerly granite, Int. J. Rock Mech. Min. Sci., 19, 49-64.

Yukutake, H., 1989, Fracturing process of granite inferred from measurements of spatial and temporal variations in velocity during triaxial deformations, J. Geophys. Res., 94, 15639-15651.

서용석
경북대학교 지질학과
702-701, 대구시 북구 산격동 1370
Tel: 053-950-6344
Fax: 053-950-5362
e-mail: ysseo@bh.kyungpook.ac.kr

정교철
안동대학교 지구환경과학과
760-749, 경북 안동시 송천동 388
Tel: 0571-850-5753
Fax: 0571-841-1627
e-mail: jeong@andong.ac.kr